

*Compensation for Self-Focusing on the OMEGA EP Laser by Use of Frequency Conversion*

**Nikhil Bose**

Sutherland High School

Advisor: Mark Guardalben

Laboratory for Laser Energetics

University of Rochester

November 2017

**1. Abstract:**

High-energy, short-pulse laser systems, such as OMEGA EP at the University of Rochester's Laboratory for Laser Energetics, must be carefully designed and operated to avoid laser-induced damage to their many optical components. OMEGA EP is a petawatt-class laser system and global resource for basic science research in high-energy-density physics.<sup>1</sup> One common pathway to damage among such laser systems is self-focusing of the laser beam caused by a nonlinear response of optical materials to high-intensity laser light. Maintaining the laser intensity below the damage threshold requires the beam size to be large, driving up the fabrication cost of optical components and increasing the design and operational complexity of the laser system. Even for large beam sizes, the maximum energy must be limited to avoid the self-focusing effect. For example, shots on the short-pulse beamlines of OMEGA EP are limited to below their maximum design energy for pulse widths of 100 ps to avoid damage from small-scale self-focusing. We have developed a simulation model to explore the use of a frequency conversion crystal that is inserted into an OMEGA EP beamline to compensate for this self-focusing. A Matlab frequency conversion model was developed and used to design a crystal whose effective nonlinear response partially cancels the nonlinear response that produces self-focusing of the beam. By incorporating this model into an OMEGA EP system model,<sup>2</sup> it was shown that a 4.5-cm DKDP crystal reduces the peak-to-mode modulation in the beam by up to 10%. This suggests that it might be possible to increase the on-target energy limit in OMEGA EP to close to its design energy for 100-ps shots.

## 2. Introduction:

On the short-pulse beamlines of OMEGA EP, shots are limited to below their maximum design energy in order to reduce the risk of damage to many of the optical components in the laser system. As the beam propagates, spatially localized regions of high intensity form across the face of the beam by the process of self-focusing, increasing the risk of damage. For 100-ps pulse widths on OMEGA EP, the self-focusing effect is greater at higher laser energies. In order to increase the beamline energy, it is necessary to limit the formation of high intensity spikes across the beam by reducing the self-focusing effect. This effect originates from the intensity-dependent refractive index of the optical components, causing small intensity modulations that initially exist across the laser beam to grow nonlinearly as the beam propagates through the laser system. Self-focusing occurs because the intensity-dependent refractive index imparts nonlinear (B-integral) phase to the beam, effectively producing localized “lenslets” across the beam where the laser beam’s phase changes rapidly.

In this work, we investigate the use of a deuterated potassium dihydrogen phosphate (DKDP) frequency conversion crystal to reduce the self-focusing effect by producing an intensity-dependent phase opposite in sign to that produced by the intensity-dependent refractive index. The crystal imparts an intensity-dependent compensating phase to the laser beam by converting the fundamental frequency of the laser to its second harmonic, and then back again to the fundamental in a cascaded frequency conversion process. In second-harmonic generation (SHG), such crystals are typically used to maximize the second-harmonic conversion efficiency by precisely aligning the crystallographic axes to the input beam direction such that the SHG process is phase-matched. In the cascaded frequency conversion process, the crystal is angularly detuned away from the phase-matched angle so that the energy, while remaining mostly in the form of the fundamental, cycles between the fundamental and second harmonic. Compensation for self-focusing by use of frequency conversion was demonstrated in BBO (beta barium borate) under very different laser conditions than exist in OMEGA EP.<sup>3</sup> The large beam size of fusion-scale lasers such as OMEGA EP constrains the choice of crystals to the KDP family of crystals, imposing unique design complexities. We show that by careful choice of crystal length and detuning angle, phase compensation and maximum fundamental wave throughput can be achieved simultaneously.

This report is organized as follows. In Section 3, we provide a background to the problem by briefly describing the origin of laser beam self-focusing and showing its effect on the OMEGA EP beam. In Section 4, the theory of the cascaded frequency conversion process is described. Section 5 discusses the crystal design methodology with considerations specific to OMEGA EP. Section 6 presents the proposed design solution and expected reduction in self-focusing. We provide concluding remarks in Section 7.

### 3. Background

Due to small-scale beam modulation, the on-target energy of Beam 2 in OMEGA EP is limited to 2300 Joules for 100-ps pulses, which is 300 J below the design energy of 2600 J. As shown by the measured near-field beam profiles in Fig. 1, small-scale beam modulation caused by self-focusing and the risk of laser damage are greater for higher energy shots when the pulse width is held constant. In Fig. 1, (a) is an image of a lower energy shot while (b) is a higher energy shot.

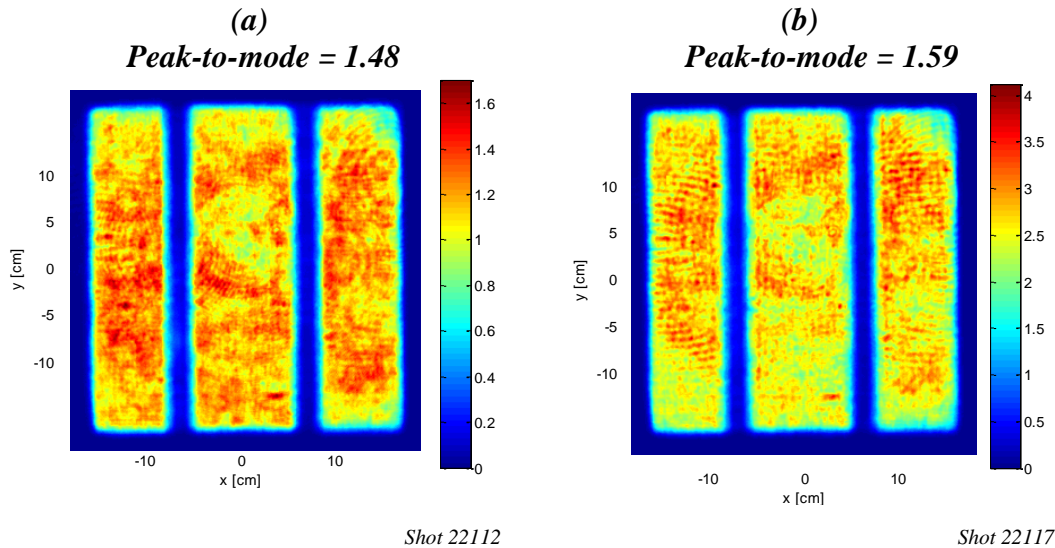


**Figure 1:** Measured near-field beam fluence of OMEGA EP Beam 2 at 100-ps pulse width at (a) low energy (1151 J) and (b) high energy (2600 J). The small-scale beam modulation, represented by the peak to mode\* fluence of the beam, and the risk of laser damage are greater for higher intensity shots. Units of fluence are  $J/cm^2$ .

\*Peak to mode is the ratio of the maximum fluence in the beam to the most common value, thus it is a good way to measure how uniformly the energy is spread across the beam.

Fig. 2 describes how the intensity dependent refractive index,  $n_2$ , can cause a laser beam to self-focus. The total refractive index can be written as

$$n = n_0 + n_2 I \quad (1)$$

where  $n$  is the refractive index,  $n_0$  and  $n_2$  are the linear and nonlinear parts of the refractive index, respectively, and  $I$  is the intensity of the light.<sup>4</sup> Eq. (1) states that as the intensity ( $I$ ) increases, the refractive index ( $n$ ) also increases. Since refractive index is a measure of the phase velocity of the light within a substance and a higher refractive index corresponds to a delay in phase, the beam's phase front is impeded at locations of higher intensity for positive values of  $n_2$ . This effect is illustrated in Fig. 2. For a beam entering a positive  $n_2$  material with an initially Gaussian intensity profile, a phase curvature is imparted to the beam's wavefront that produces an intensity spike at its center upon further propagation (Fig. 2c). Phase is accumulated via the B-integral phase equation:

$$B(x, y) = \frac{2\pi}{\lambda} \sum_{optics} n_2 L_{optic} I_{optic}(x, y) \quad (2)$$

where  $\lambda$  is the wavelength,  $L_{optic}$  is the length of the optic, and  $I_{optic}(x, y)$  is the intensity of the beam at the point  $(x, y)$ .

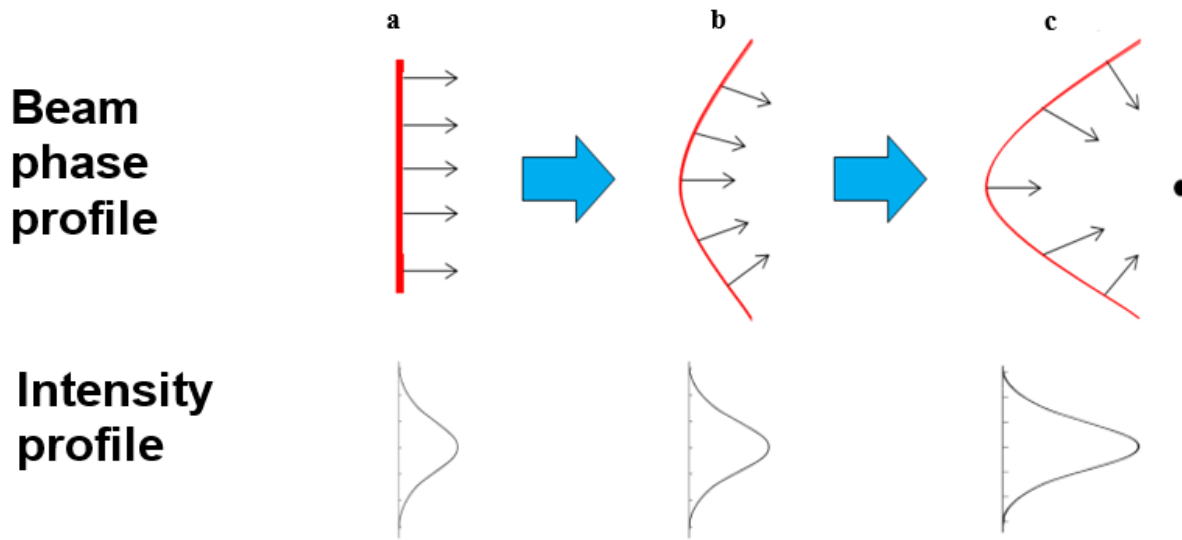


**Figure 2:** Phase and intensity profile for a beam showing the effect of the B-integral phase. As the beam propagates, the energy becomes more concentrated at the center due to self-focusing. (a) The phase front is initially flat and the intensity is initially Gaussian. (b) As the beam propagates, the beam's phase is impeded at locations where the intensity is higher due to the intensity-dependent refractive index. Since the direction of propagation is perpendicular to the beam's phase front, the energy gets more concentrated at the beam's center. (c) Further self-focusing occurs with propagation where the risk of damage to many of the optical components of the laser is high.

In addition to this whole beam self-focusing effect, small-scale self-focusing can occur if the beam contains localized regions of higher and lower intensity. For example, diffraction

around dust particles on the surfaces of optical components in OMEGA EP produces intensity modulation that can seed the self-focusing process.

#### 4. Theory of Cascaded Frequency Conversion

In phase-matched SHG, the phase relationship between an input fundamental wave and its generated second harmonic is fixed such that maximum conversion efficiency is achieved. As shown in Fig. 3, in non-phase-matched (e.g., angularly detuned) SHG, the input beam, while remaining mostly as the fundamental, cycles between its fundamental frequency and its second harmonic frequency as it propagates through the crystal. The rate at which this cycling occurs is intensity dependent. This periodic energy exchange between the fundamental wave and the second harmonic wave produces a corresponding intensity-dependent nonlinear phase shift in the fundamental wave.<sup>5</sup> Because the process is not phase matched, the second harmonic travels at a different phase velocity with respect to the fundamental. Thus, when the second harmonic converts back to the fundamental, the resulting fundamental wave will have a different phase from the original beam had it not undergone the conversion to the second harmonic and back but instead had traveled the same distance.<sup>5</sup> The resulting phase difference is intensity dependent, and can either add to or decrease the accumulated phase on the original beam.<sup>5</sup> A type-I frequency conversion crystal can be designed such that the change in phase has the opposite sign of the intensity-dependent B-integral phase that is initially on the fundamental wave. Since both processes are intensity dependent, phase perturbations on the fundamental beam leading to self-focusing can be selectively reduced in regions where B-integral phase is large.



**Figure 3:** Illustration of the cascaded SHG process in a type-I nonlinear crystal, such as DKDP. The red beam represents the fundamental wave and the green beam represents its second harmonic.  $E_1$ ,  $\lambda_1$ , and  $E_3$ ,  $\lambda_3$  respectively represent the electric field amplitudes and wavelengths of the beams. For non-phase-matched conditions, periodic energy exchange occurs between the two waves, producing an intensity-dependent nonlinear phase shift in the fundamental wave.

The frequency conversion process is governed by the coupled wave equations, Eq. (3) and Eq. (4), that describe the evolution of the fundamental and second harmonic slowly varying electric field amplitudes ( $E_1$  and  $E_3$ , respectively) with propagation distance,  $z$ , in the crystal.<sup>5</sup> In Eqs. (3) and (4),  $E_1$  and  $E_3$  are normalized such that  $|E_1|^2$  and  $|E_3|^2$  are the respective irradiances of the two waves. The other parameters in these equations and their values used in the DKDP crystal design process are given in Table 1. The first two terms on the right-hand side of Eqs. (3) and (4) represent absorption and the SHG process, respectively. The third term in Eq. (3) accounts for the change in refractive index due to the intensity of the fundamental.

$$\frac{dE_1}{dz} = -\frac{1}{2}\gamma_1 E_1 - i\kappa E_3 E_1^* e^{i\Delta kz} - i \frac{3\omega}{(cn)^2 \epsilon_0} \chi_{eff}^{(3)} |E_1|^2 E_1 \quad (3)$$

$$\frac{dE_3}{dz} = -\frac{1}{2}\gamma_3 E_3 - i\kappa E_1^2 e^{-i\Delta kz} \quad (4)$$

Parameter	Definition	Value <sup>6</sup>
$\gamma_1$	Absorption coefficient of fundamental	0.021 cm <sup>-1</sup>
$\gamma_3$	Absorption coefficient of second harmonic	0.001 cm <sup>-1</sup>
$\omega$	Angular frequency of fundamental	1.7871e15 rad/s
$\kappa$	Nonlinear coupling coefficient	9.9512e-06 sec <sup>1/2</sup> /J <sup>1/2</sup>
$\chi_{eff}^{(3)}$	Third-order optical susceptibility of fundamental	3e-23 m <sup>2</sup> /V <sup>2</sup>
$\Delta k$	Phase mismatch between fundamental and second harmonic	256.76 m <sup>-1</sup>
$\epsilon_0$	Permittivity of free space	8.8541e-12 F/m
$c$	Speed of light in vacuum	2.9979e8 m/s
$n$	Refractive index of fundamental	1.4935

**Table 1:** Definitions of parameters in Eqs. (3) and (4) and their values used in the DKDP crystal design process. Values of  $\Delta k$  and  $\kappa$  are those for angular detuning of 0.55 mrad from the phase matched angle. The fundamental angular frequency shown corresponds to the wavelength of 1054 nm. The value for  $\gamma_1$  was calculated using a weighted average for KDP and 99% deuterated KDP, assuming the typical value of 70% deuteration level for the crystal size and cut required.

In Eqs. (3) and (4), the phase mismatch between fundamental and second harmonic ( $\Delta k$ ) can be expressed as,

$$\Delta k = 2 * k_1 - k_3 \quad (5)$$

where  $k_1$  and  $k_3$  are the wave numbers of the fundamental and the second harmonic, respectively. Since,

$$k = \frac{n*\omega}{c} \quad (6)$$

where  $n$  is the refractive index,  $\omega$  is the angular frequency, and  $c$  is the speed of light, Eq. (5) can be expressed as,

$$\Delta k = 2 * \frac{n_1 * \omega_1}{c} - \frac{n_3 * 2 * \omega_1}{c} = \frac{2 * \omega_1}{c} * (n_1 - n_3) \quad (7)$$

where  $n_1$  and  $n_3$  are the refractive indices of the fundamental and second harmonic, respectively. Since this is type-I frequency conversion,  $E_1$  is an ordinary wave whereas  $E_3$  is an extraordinary wave. This means that as the detuning angle changes,  $n_1$  does not change while  $n_3$  does. Thus, in this setup,  $\Delta k$  is proportional to the detuning angle. This means that by changing the detuning angle the rate of energy transfer between the waves and their relative phases can be changed.

A frequency conversion model was developed using Eqs. (3) and (4), and used as a subroutine in an OMEGA EP beamline model<sup>2</sup> to test different crystal configurations, as discussed in Sections 5 and 6. The subroutine works by modeling all points across the laser beam as it travels through the frequency conversion crystal and by assuming the pulse is flat in time of width 1.2 ns. This pulse width is approximately equal to the width of the pre-compressed pulse in the OMEGA EP beamline, described in Section 6.

## 5. Design Considerations and Methodology

When designing a crystal to compensate for the self-focusing effects on OMEGA EP, one must consider the limited commercial availability of sufficiently large aperture nonlinear crystals that would accommodate the OMEGA EP beam size of approximately 36 cm x 36 cm. The only suitable crystals available at this size are the KDP family of single crystals grown from aqueous solution of component salts. Thus, principal design considerations were crystal length ( $L$ ) and detuning angle for the expected intensity level in the OMEGA EP beamline. Fig. 4 shows (a) the beam intensity and (b) the nonlinear phase for four different detuning angles as the beam goes through the crystal. The four different detuning angles and their corresponding values of  $dkL$  (the product of  $\Delta k$ , given by Eq. (5), and the crystal length), are shown in the key. As seen in Fig. 4, the detuning angle and crystal length are coupled such that only discrete crystal lengths provide maximum fundamental wave throughput for a given input intensity and amount of detuning. In addition, a trade-off exists among the choices of crystal length, detuning angle, and amount of compensating phase. Since maximum fundamental throughput is required, only crystal lengths very close to the peaks of the different intensity curves in Fig. 4(a) can be selected. For example, the red dashed line in Fig. 4(a) is drawn at the peak of the curve for a

detuning of 0.55 mrad (the “moderate detuning” in Fig. 4), so the corresponding crystal length of 44 mm can be considered. With this choice of crystal length and detuning, Fig. 4(b) indicates that approximately  $-0.12\pi$  radians of accumulated phase can be achieved. In order to reduce crystal fabrication costs and sensitivity to alignment in the laser system, it is desirable to have crystal lengths within the range of approximately 10 mm – 45 mm. In Fig. 4(a), as the detuning angle increases, more crystal lengths within the 10 mm – 45 mm range offer maximum transmission, but Fig. 4(b) shows that the accumulated nonlinear phase is correspondingly smaller. Thus, a detuning angle of 0.55 mrad was selected, which allowed for sufficient phase compensation while also providing the choice of reasonable crystal lengths (22 – 24 mm and 43 – 45 mm). It is important to note that Fig. 4 is derived using a single beam intensity while OMEGA EP’s beams have intensity variations. Thus, while the crystal lengths that correspond to maximum transmission in Fig. 4 are good starting points, they may vary slightly from the optimal solution for OMEGA EP. To show the locations of maximum energy transmission clearly, the plots in Fig. 4 do not take the absorption of the crystal into account. However, DKDP was selected due to its lower absorption coefficient compared to other KDP family crystal choices.

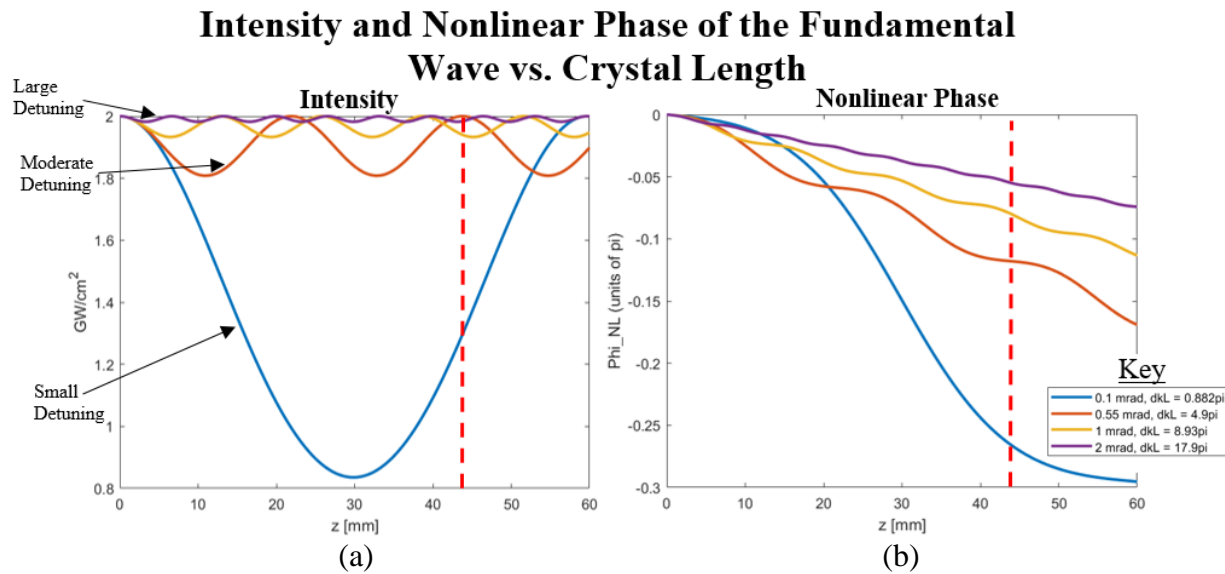


**Figure 4:** Plots of (a) output intensity and (b) the accumulated nonlinear phase of the fundamental wave vs. the length of DKDP crystal. These plots were made using Eqs. (3) and (4), but without the absorption term to illustrate the primary considerations in the design optimization process. For maximum output energy in the fundamental wave, a trade-off exists among crystal length, tilt angle, and nonlinear phase. The vertical dashed line identifies one design solution that requires a crystal length of 44 mm and tilt angle of 0.55 mrad to achieve approximately  $0.12\pi$  radians of nonlinear phase. Input intensity to the crystal used in these plots is  $2 \text{ GW/cm}^2$ , and is close to the maximum beamline intensity after the last path through the booster amplifiers (see Fig. 5).

The amount of phase compensation that is necessary to compensate the B-integral phase is dependent on the location of the crystal in the beam's path. The localized "lenslets" across the beam, produced by the B-integral phase, vary in size. The amount of phase compensation must match the amount and local size of the B-integral regions for the compensation to be effective. Early in the beam's path the lenslets are essentially non-existent because, at this point, the laser beam has very little B-integral phase. As the beam propagates, the intensity modulations and lenslets change in size and the overall intensity gets higher. To account for this, locations early and late in the beam's path were investigated.

## 6. Proposed Design Solution

The OMEGA EP short-pulse beams are generated through two of its four beamlines. A schematic of the portion of one beamline relevant to this investigation is shown in Fig. 5, illustrating the major optical components, the laser beam's path, and the three crystal locations investigated. The laser pulse is injected into the beamline from a separate laser source location toward the 7-disk booster amplifier and the 11-disk main cavity amplifier, where it sees significant amplification of its energy. After making four passes through the main cavity, the laser pulse is switched out of the main cavity, making a second pass through the booster amplifier. The laser pulse then propagates through several optical components on its way to the target, including a grating pulse compressor and off-axis parabola focusing mirror (not shown in Fig. 5) that respectively compress the laser pulse in time and focus it onto the target.

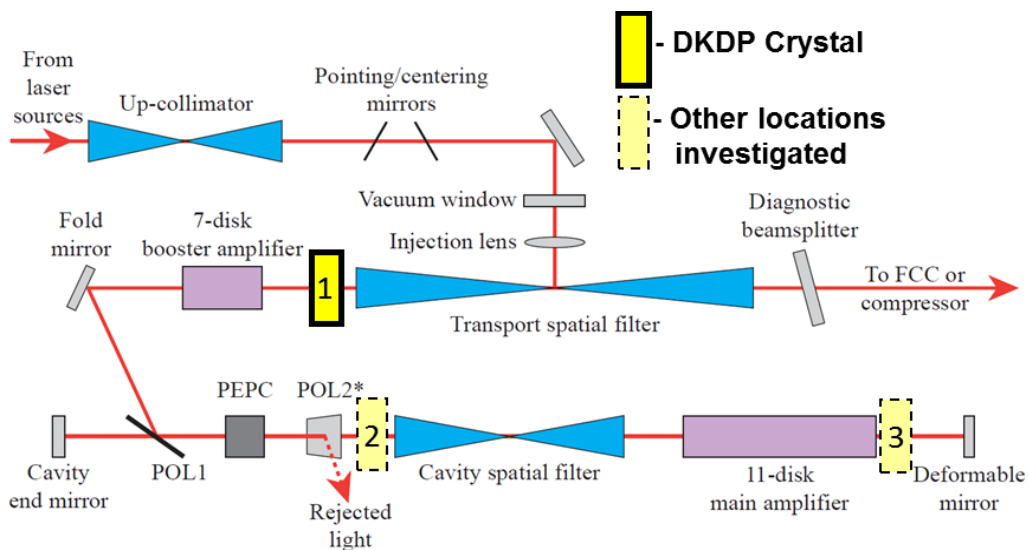


**Figure 5:** Schematic of the OMEGA EP beamline showing the three locations for the DKDP crystal that were investigated (also see Table 2).

Table 2 provides a summary of why the three locations shown in Fig. 5 were chosen for investigation. The more times the beam passes through the crystal the more opportunities there are for the crystal to impart phase, and the higher the intensity on each pass the more compensating phase is imparted. However, there is a trade-off between the number of times the beam passes through the crystal and the beam's intensity. This is because the beam passes through the crystal four times at locations 2 and 3, as opposed to 2 times at location 1, but the beam reaches its highest intensity just before its last pass of location 1.

Location	Description	Motivation
1	Between the transport spatial filter and booster amplifiers	<ul style="list-style-type: none"> <li>Higher intensity in a single pass than locations 2 and 3 owing to final pass through booster amplifiers</li> </ul>
2	Between polarizer 2 (POL2) and the cavity spatial filter	<ul style="list-style-type: none"> <li>Main cavity allows four passes through crystal, potentially providing greater accumulated nonlinear phase than location 1</li> <li>Lower single-pass intensity than location 1, but higher than location 3 on final pass of main cavity</li> </ul>
3	Between the main amplifiers and the deformable mirror	<ul style="list-style-type: none"> <li>Main cavity allows four passes through crystal</li> <li>Close to image plane located at the deformable mirror*</li> <li>Beam's intensity is higher during its first and third pass of the crystal but lower during the second and fourth compared to location 2.</li> </ul>

**Table 2:** Different locations tested for placement of DKDP crystal nonlinear phase compensator in the OMEGA EP beamline and motivation for each choice. Location 1 provided the greatest amount of compensating phase because of the high input intensity to the crystal on the beam's final pass, and produced the greatest reduction in downstream self-focusing among the three locations investigated, as described in the text.  
\*In general, beam modulation gets worse as the beam gets farther away from an image plane. Thus, by placing the crystal near an image plane, the relative contribution of imaging to the phase compensation can be investigated.

Plots similar to those shown in Fig. 4 were used to choose possible crystal lengths and angular detunings. For each choice of crystal length, detuning, and crystal location in the beamline, the OMEGA EP system model<sup>2</sup> was used to calculate the beam's intensity modulation at several locations along the beam path. Through this process, a 4.5-cm DKDP crystal at location 1 in Fig. 5, detuned by 0.55 mrad, was determined to achieve the greatest phase compensation while also minimizing residual second harmonic light.

Fig. 6 shows the beam's peak-to-mode value and its maximum intensity for the beam's final pass through the beamline, where the vertical red line in the figure represents the location where the beam makes its second pass through the compensator. Without the crystal, the on-target energy was 2520 J. To compensate for the absorption of energy by the crystal, the input energy to the beamline was increased when the crystal was inserted into the beamline to produce

comparable on-target energy of 2510 J. This higher injected energy is apparent in the beam's higher maximum intensity before the second pass through the crystal (left of the vertical red line in Fig. 6(b)). After passing through the crystal, however, Fig. 6 shows that both the beam's peak-to-mode modulation and maximum intensity are significantly reduced at all subsequent beamline locations (right of vertical red line in Fig. 6). Maximum intensity in the beam is reduced at components most susceptible to laser damage, which include the fourth grating of the grating pulse compressor and those components downstream of this grating (UC G4 and components to the right of UC G4 in Fig. 6). The higher intensity in the region of the beamline to the left of the vertical red line in Fig. 6 when the crystal is inserted is well below the damage threshold for these optical components.

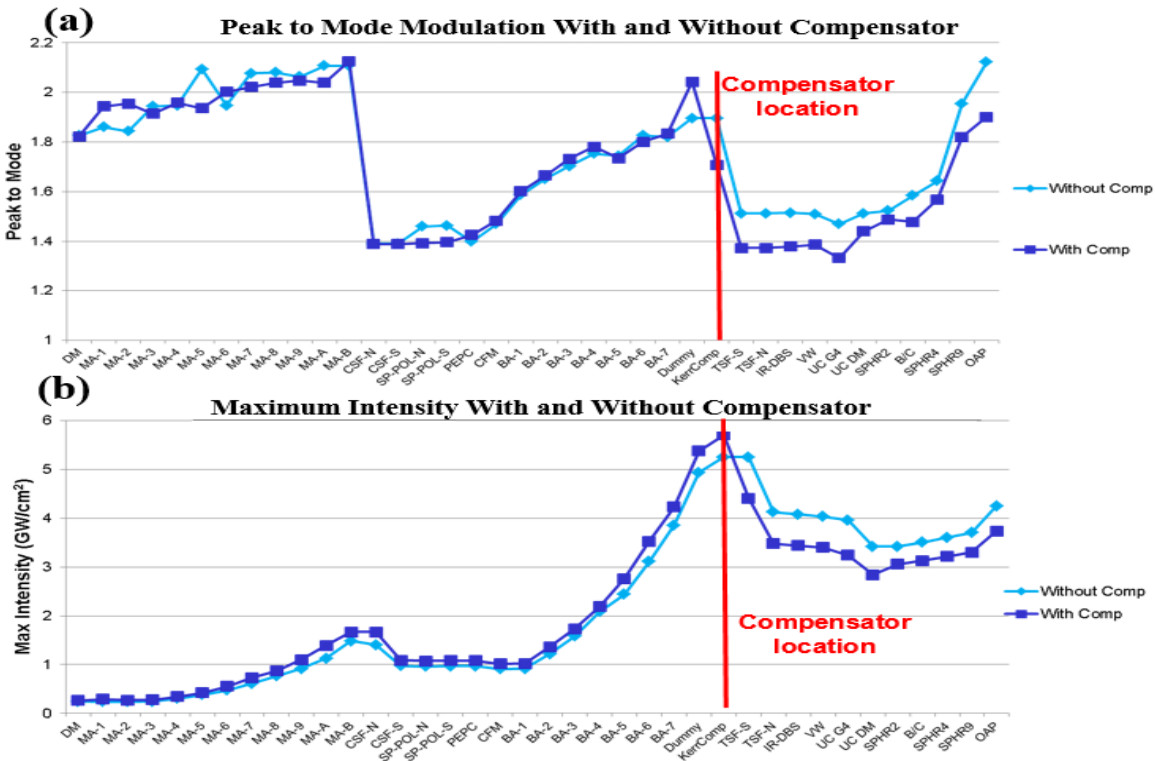


**Figure 6:** Plots of (a) peak-to-mode and (b) maximum intensity of the beam at the output of successive beamline components for the last pass through the beamline starting at the deformable mirror, with and without the crystal compensator. The beam's path is from the left to the right in the plots. The red line indicates the location of the compensator (location 1 in Fig. 5). Components most susceptible to laser damage include UC G4 and those to the right of UC G4 in the plots. DM – deformable mirror, MA-1 through MA-B – 11 disks of main amplifiers, CSF-N and CSF-S – ends of cavity spatial filter, SP-POL-N and SP-POL-S – ends of short-pulse polarizer, PEPC – plasma-electrode Pockels cell, CFM – cavity fold mirror, BA-1 through BA-7 – 7 disks of booster amplifiers, Dummy – empty optic inserted to allow OMEGA EP model to continue diffraction of the beam until it reaches the crystal, KerrComp – frequency conversion crystal, TSF-S and TSF-N – ends of transport spatial filter, IR-DBS – diagnostic beam splitter, VW – vacuum window, UC G4 – fourth grating of upper compressor, UC DM – upper compressor deformable mirror, SPHR2 – short pulse high reflector 2, B/C – beam combiner, SPHR4 and SPHR9 – short pulse high reflectors 4 and 9, OAP – off-axis parabola.

The compensating phase generated by the DKDP crystal is shown in Fig. 7 for one case. At the vacuum window (VW in Fig. 6), without phase compensation, the average B-integral phase across the beam was approximately 2.5 radians (Fig. 7(a)). With the phase compensation crystal, the average phase at the vacuum window was reduced to approximately 1.8 radians (Fig. 7(b)). This reduction in phase was due to phase of opposite sign from the crystal of approximately -0.7 radians (Fig 7(c)).

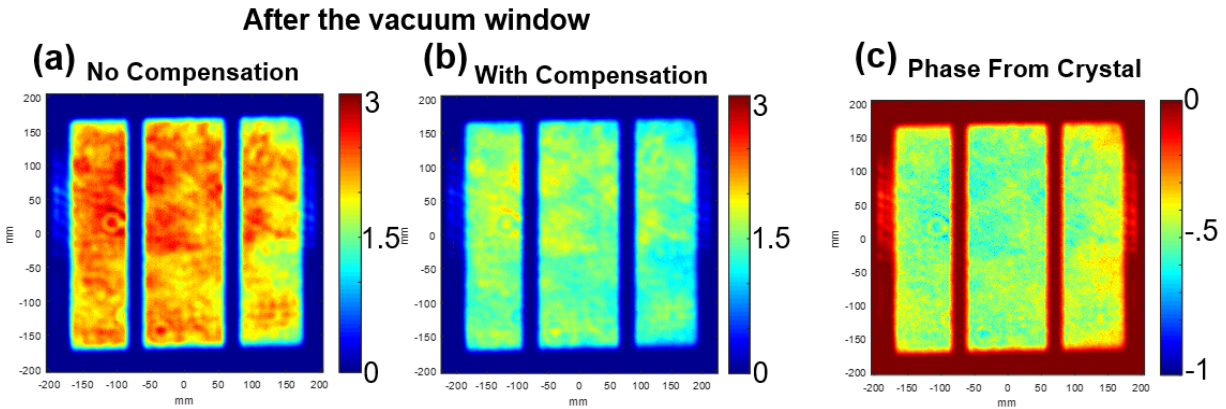


**Figure 7:** Calculated near-field beam accumulated phase in radians at the vacuum window. (a) B-integral phase without the DKDP crystal compensator; (b) beam phase with the DKDP crystal compensator at location 1. Phase of opposite sign imparted by the crystal is shown in (c). Regions in the beam shown in (a) that have higher B-integral phase also have greater compensating phase in (c).

Shown in Fig. 8 are the near-field images and peak-to-mode (P:M) values of the beam at the compressor vacuum window, the UC G4 grating, and the off-axis parabola with and without the compensator. These key elements are very expensive and difficult to replace, thus damage to them is of great concern when increasing the on-target energy of the beam. In the simulation, there is a significant smoothing effect on the beam when the crystal is inserted into the beamline due to a reduction in the self-focusing effect. This is shown in Fig. 8 by the decrease in the peak-to-mode at these locations by up to 10%, compared to simulations without the crystal.

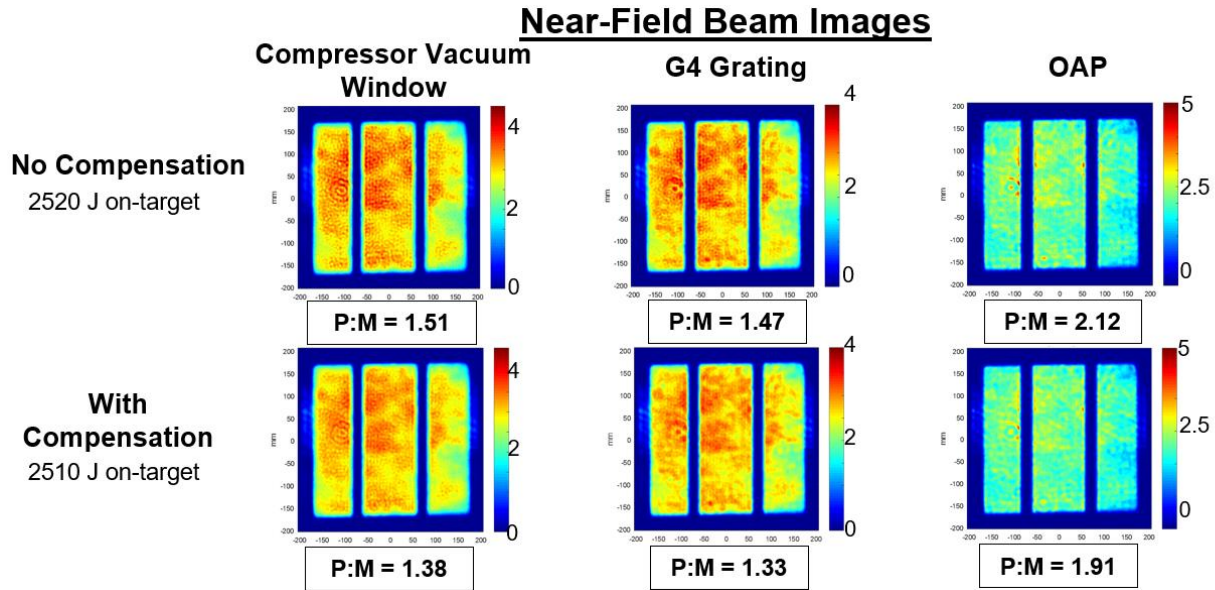


**Figure 8:** Calculated near-field images of the beam at the compressor vacuum window, the G4 grating, and the off-axis parabola (OAP). The images represent the fluence of the beam which is a measure of energy per unit area and has units of  $J/cm^2$ . Significant smoothing of the beam is seen with the compensating crystal inserted, owing to a reduction in self-focusing.

Since the amount of phase compensation and residual second harmonic conversion is dependent upon the angular detuning of the crystal, the sensitivity of the crystal to angular alignment errors is an important consideration in its design. Other frequency conversion crystals designed for high conversion efficiency in OMEGA EP are routinely maintained at crystal angles to within  $\pm 0.025$  mrad of peak conversion, and beam wavefront errors typically have gradients of up to approximately 0.015 mrad. Thus, we investigated the sensitivity of the compensating crystal to comparable changes in the detuning angle, as shown in Fig. 9, where the normalized fundamental wave energy and the peak-to-mode values at the OAP are plotted for a range of detuning angles about the design angle of 0.55 mrad. Within a range of  $\pm 0.05$  mrad, the fundamental wave energy varied by only 6%, while the peak-to-mode ranged from 1.85 to 2.00. These relatively small changes suggest that small alignment errors or beam wavefront errors will not be a major impediment to successful deployment of a phase compensator in the laser system.

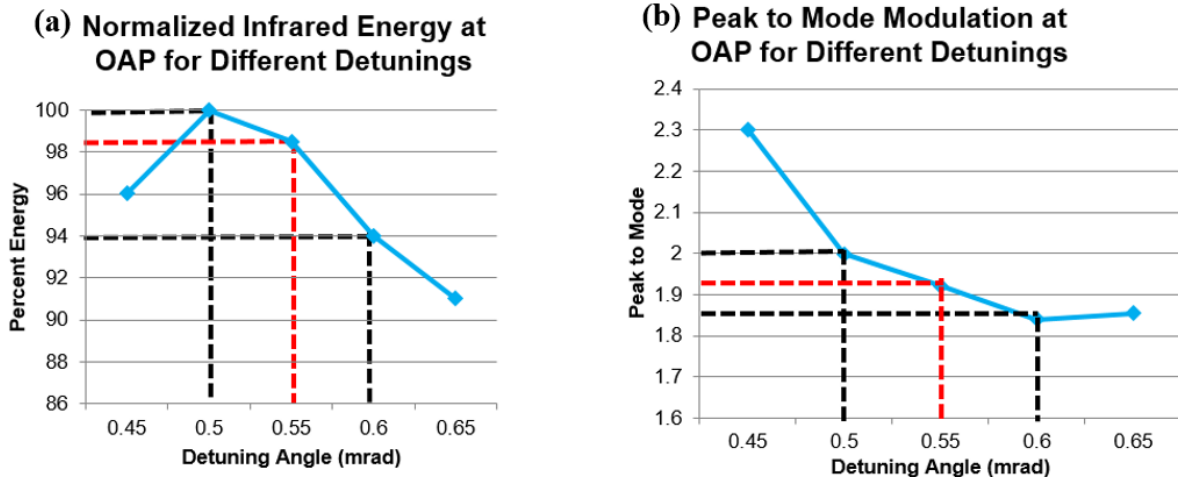


**Figure 9:** a) Normalized energy and b) beam modulation at the OAP vs. crystal detuning angle showing the sensitivity of the crystal to angular alignment and beam wavefront errors. The red dashed line shows the design 0.55 mrad while the black dashed lines show the bounds of the  $\pm 0.05$  mrad range.

## 7. Conclusion

In this work we explored the use of a frequency conversion crystal to compensate for self-focusing on 100-ps laser shots in OMEGA EP. A MATLAB frequency conversion model was used to design a crystal whose effective nonlinear response partially compensates for the self-focusing effects of the beam. This model was incorporated into an OMEGA EP system model<sup>2</sup> to simulate the effects of frequency conversion crystals within the OMEGA EP beam path. Based on these simulations, it was determined that a 4.5-cm DKDP crystal, detuned by 0.55 mrad and placed between the booster amplifiers and transport spatial filter, achieved the best results. With the crystal inserted into the beamline, the beam modulation was reduced by approximately 10% at optical components most susceptible to laser damage. These results suggest that it may be possible to increase the on-target energy on the short-pulse beamlines of OMEGA EP from 2300 J to close to the design energy (2600 J) for 100-ps shots with the use of a DKDP compensator.

## 8. Acknowledgements

I would like to thank my advisor, Mark Guardalben, for all his advice, time, and help. I would also like to thank Dr. R. Stephen Craxton and the Laboratory for Laser Energetics for giving me this wonderful opportunity to spend my summer doing research and Dr. B. Kruschwitz

for creating the OMEGA EP beamline model into which I incorporated my frequency conversion model.

## References

---

1. University of Rochester - Laboratory for Laser Energetics - OMEGA EP, [www.ile.rochester.edu/omega\\_facility/omega\\_ep/](http://www.ile.rochester.edu/omega_facility/omega_ep/).
2. MATLAB OMEGA EP SP model provided courtesy of Dr. Brian Kruschwitz.
3. Beckwitt, Kale, et al. "Compensation for Self-Focusing by Use of Cascade Quadratic Nonlinearity." *Optics Letters*, vol. 26, no. 21, pp. 1696–1698, 2001.
4. Roth, Ulrich, et al. "Compensation of Nonlinear Self-Focusing in High-Power Lasers." *IEEE Journal of Quantum Electronics*, vol. 36, no. 6, pp. 687–691, 2000.
5. Stegeman, George I. "Cascading: Nonlinear Phase Shifts." *Quantum and Semiclassical Optics: Journal of the European Optical Society Part B*, vol. 9, no. 2, pp. 139–153, 1997.
6. Values for  $\gamma_1$  and  $\gamma_3$  from Dimitriev, Valentin G., et al. "Handbook of Nonlinear Optical Crystals". Springer. 1999.  
Value for  $\chi_{eff}^{(3)}$  is estimated from Ganeev, R. A. "Characterization of Nonlinear Optical Parameters of KDP, LiNbO<sub>3</sub>, and BBO Crystals." *Optics Communications*, vol. 229, pp. 403–412, 2004.